BEST AVAILABLE IMAGES

Defective images within this document are accurate representations of the original documents submitted by the applicant.

Defects in the images may include (but are not limited to):

- BLACK BORDERS
- TEXT CUT OFF AT TOP, BOTTOM OR SIDES
- FADED TEXT
- ILLEGIBLE TEXT
- SKEWED/SLANTED IMAGES
- COLORED PHOTOS
- BLACK OR VERY BLACK AND WHITE DARK PHOTOS
- GRAY SCALE DOCUMENTS

IMAGES ARE BEST AVAILABLE COPY.

As rescanning documents *will not* correct images, please do not report the images to the Image Problem Mailbox.

PROCEEDINGS
SPIE—The International Society for Optical Engineering

International Lens Design Conference

George N. Lawrence
Editor

11-14 June 1990
Monterey, California

Cosponsored by
Optical Society of America
SPIE—The International Society for Optical Engineering

Published by
SPIE—The International Society for Optical Engineering
P.O. Box 10, Bellingham, Washington 98227-0010 USA

Volume 1354

The papers appearing in this book comprise the proceedings of the meeting mentioned on the cover and title page. They reflect the authors' opinions and are published as presented and without change, in the interests of timely dissemination. Their inclusion in this publication does not necessarily constitute endorsement by the editors or by SPIE.

Please use the following format to cite material from this book:
Author(s), "Title of Paper," *International Lens Design Conference,* George N. Lawrence, Editor, Proc. SPIE 1354, page numbers (1990).

Library of Congress Catalog Card No. 90-50807
ISBN 0-8194-0415-2

SPIE—The International Society for Optical Engineering
P.O. Box 10, Bellingham, Washington 98227-0010 USA
Telephone 206/676-3290 (Pacific Time) • Fax 206/647-1445

Printed in the United States of America.

INTERNATIONAL LENS DESIGN CONFERENCE

Volume 1354

CONTENTS

(continued)

The design of achromatized hybrid diffractive lens systems

Carmiña Londoño and Peter P. Clark
Polaroid Corporation, Optical Engineering Department
38 Henry Street, Cambridge, MA 02139

1. Abstract

The design of two broadband hybrid diffractive-refractive optical systems, a landscape type lens and a Schmidt telescope, was investigated. The systems were achromatized using the large negative dispersion characteristic of kinoforms. In the scalar wave regime, these structures can approach 100% efficiency for one object point and wavelength, but efficiency inevitably decreases when these parameters change. We evaluated polychromatic image quality, taking diffraction efficiency into account, by constructing properly weighted geometric point spread functions from several diffracted orders and calculating modulation transfer functions.

The MTF's of the hybrid achromats were improved at high spatial frequencies, but reduced at low frequencies because inefficiency caused diffraction into non-design orders.

2. Introduction

The concept of using optical elements whose characteristic function is determined by diffraction is not new. Diffractive Optical Elements (DOE's) are based on the principles of the well known Fresnel zone plate, first constructed by Lord Rayleigh in 1871, and described by Soret in 1875[1,2]. Kinoforms[3] are surface relief phase DOE's, sometimes described as phased Fresnel lenses. They can be designed to approach 100% efficiency for a certain wavelength, diffracted order and geometry. A change in any of these parameters reduces the diffraction efficiency.

DOE's have resurfaced in the literature due to improved fabrication techniques which make them practical for use in optical systems. They are of interest to lens designers because of their unusual properties, such as very large negative dispersion and zero Petzval sum contribution. In sections 3 to 6 of this paper we discuss an approach which takes diffraction efficiency into account at the design stage. In section 7 we present the results of image quality evaluations for two design examples.

3. Hybrid Design Approach

The design of a hybrid system consists typically of minimizing the aberrations over the aperture, field of view and spectral bandwidth. The design of kinoforms can be divided into two parts. The first part is the design of the frequency distribution of the kinoform to make the wavefront error for one particular diffractive order (the "design order") acceptably small. The second part of the design is to maximize the diffraction efficiency by optimizing the form of the kinoform facets.

4. Blazed Grating Geometric Model

One can trace rays through a kinofrom by treating it as a linear blazed diffraction grating whose frequency, orientation, and blaze angle vary continuously over the surface. An enlarged detail of a kinoform's surface relief profile is shown in Fig 1. Let us consider a ray entering this hybrid grating geometry at angle θ. Ignoring the periodic structure, the ray simply refracts according to Snell's law:

$$n \sin(\alpha-\theta) = n' \sin(\alpha-\theta_0) , \qquad (1)$$

where θ_0 is simply the direction of the zero order. The prism angle, α, is determined by the base curvature of the kinoform. When the periodic grating structure is included, the ray diffracts into orders

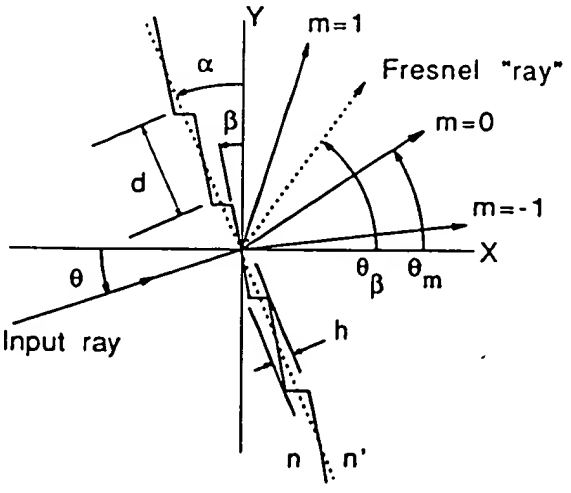

Figure 1. Hybrid (refractive and diffractive) blazed grating model of a kinoform.

whose angular separation is a function of λ, θ, α and the grating's orientation and frequency (1/d) at the ray's intercept:

$$d\,[n \sin(\alpha-\theta) - n' \sin(\alpha-\theta_m)] = m\lambda \tag{2}$$

If the grating period is large compared to the wavelength, polarization effects can be ignored and efficiency does not have to be calculated from the vector electromagnetic theory, but can instead be calculated from the simpler scalar approximation. As a general rule, the scalar theory is applicable when the groove spacing is greater than five times the wavelength, see for example Hutley[4] and Swanson[5]. The diffraction efficiency envelope for a linear grating is then the Fourier transform of the transmission function over one period, which for a linear phase grating or a kinoform is a shifted sinc^2 [$\text{sinc}(x) = \sin(x)/x$]. The center of the efficiency envelope, θ_β is geometrically determined by the refraction of the input ray, as a function of β:

$$n \sin(\beta-\theta) = n' \sin(\beta-\theta_\beta) \tag{3}$$

From this geometrical model, it can be seen that the design of the grating frequency distribution is separate from the design of its diffraction efficiency. To design a phase grating with order m 100% efficient, the proper blaze angle (β) must be chosen to make θ_β equal θ_m. If a specific diffracted ray matches the refraction of the blaze, the efficiency of that diffracted order is 100%, because the envelope is centered on it. Note that changing λ or θ results in new order separations and a new center for the efficiency envelope. In particular, for a broadband system there may be a significant amount of light diffracted into non-design orders.

To calculate the efficiency of a broadband kinoform, the efficiency function for a blazed linear grating or a kinoform may be written in the small angle (low-frequency grating) approximation as:

$$\varepsilon(m,\lambda) = \text{sinc}^2\left[\pi\left(m - m_0 \frac{\lambda_0}{\Delta n(\lambda_0)} \frac{\Delta n(\lambda)}{\lambda}\right)\right], \qquad \text{where} \quad \Delta n(\lambda) = n'(\lambda) - n(\lambda), \tag{4}$$

and λ_0 and m_0 are the wavelength and order for which the design is 100% efficient. The height of the blaze, h, is related to λ_0 and m_0 by:

$$h = d\,(\alpha - \beta) = m_0 \frac{\lambda_0}{\Delta n(\lambda_0)}\,. \tag{5}$$

Equation (4) was used to generate Fig.2, a histogram of efficiency vs. diffracted order for a linear phase grating or a kinoform, designed to be 100% efficient for the first order at λ=550 nm. For wavelengths other than 550 nm, the first order (m=1) efficiency is less than 100%. Consider for example, if λ changes from 550 nm to 400 nm, the efficiency drops to 62% for m=1 while going up to 22% for m=2 and 5% for m=0.

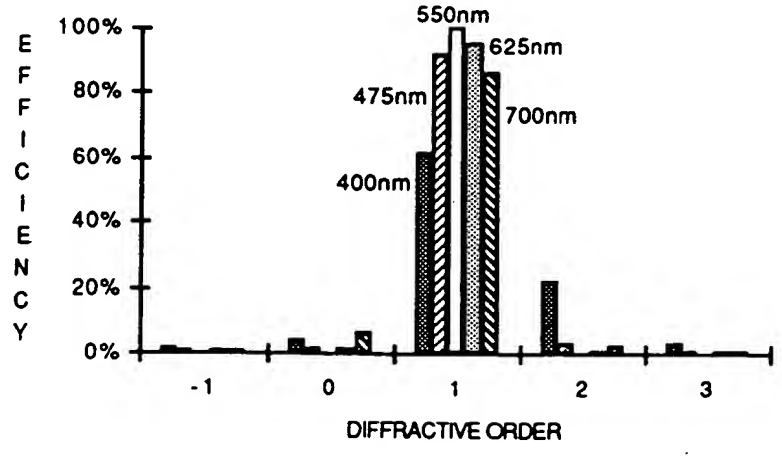

Figure 2. Diffraction efficiency variation with order and wavelength.

5. Designing Hybrid Systems

The first step of the design process is to optimize the system's image quality using the light that is diffracted in the design order by varying the lens and DOE construction parameters (surface shapes, thicknesses, etc., and the DOE's frequency distribution.) Most large lens design programs allow the designer to perform ray tracing and optimizing of diffractive optical elements, either with a special surface type (like "HOE" in CODE-V[6]) or by using Sweatt's high refractive index model[7]. These ray tracing techniques can be used to determine the paths of diffracted rays of any order.

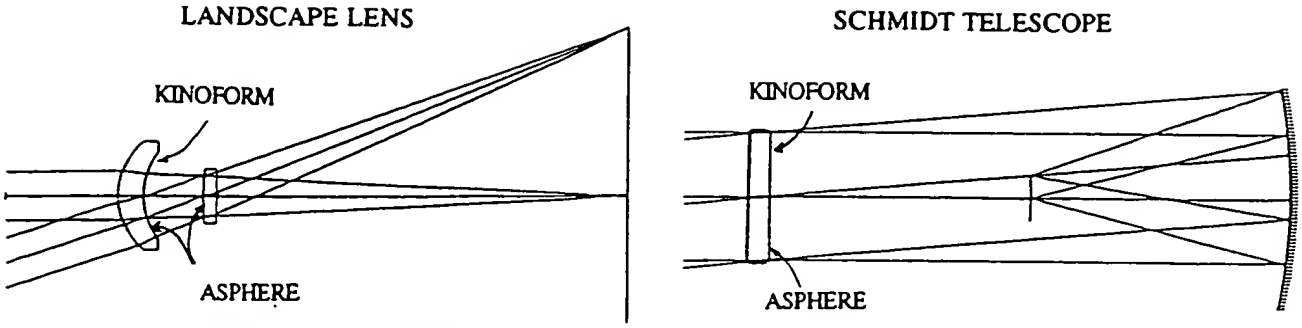

Material	Acrylic (PMMA)
n_d	1.4917
$V_{F,C}$	57.2
EFL	114.3 mm
f/number	9.2
Field of view	±18°
Δλ (narrow)	656, 588, 546 nm
Δλ (wide)	656, 588, 486 nm

Material	BK7
n_d	1.5168
$V_{F,C}$	64.2
EFL	500 mm
f/number	2.0
Field of view	±5°
Δλ (narrow)	656, 588, 486 nm
Δλ (wide)	852, 588, 480 nm

Figure 5. Two design examples of hybrid achromatized systems.

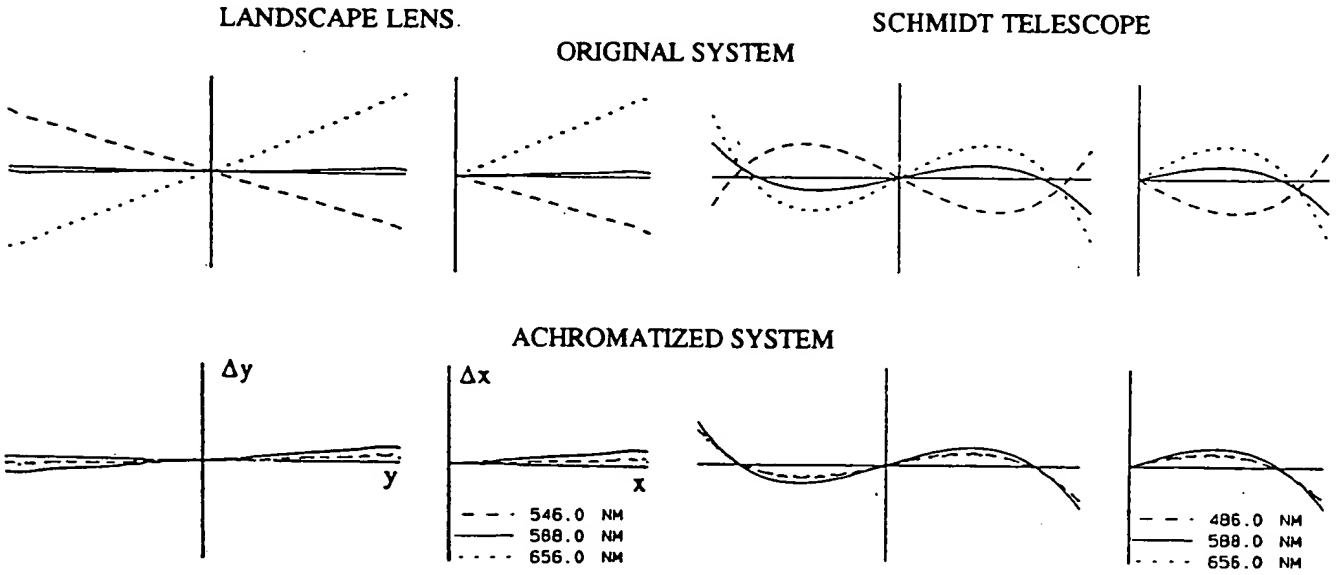

Figure 6. On-axis transverse ray aberration for the design order (m=1).

7. Image Quality Results

Schematics and specifications of the two hybrid systems used here as examples are shown in Fig.5. For the landscape lens, the DOE was used to correct the primary lateral and longitudinal chromatic aberrations. For the Schmidt the DOE corrected primary spherochromatism.

Fig.6 shows the on-axis transverse ray aberration plots for the two corrected hybrid systems with m=1. It was possible to correct both systems for primary color aberrations. However, notice the residual secondary color in the landscape lens and secondary spherochromatism in the Schmidt telescope. These plots show the aberration correction of the design order, but not the effects of diffraction efficiency.

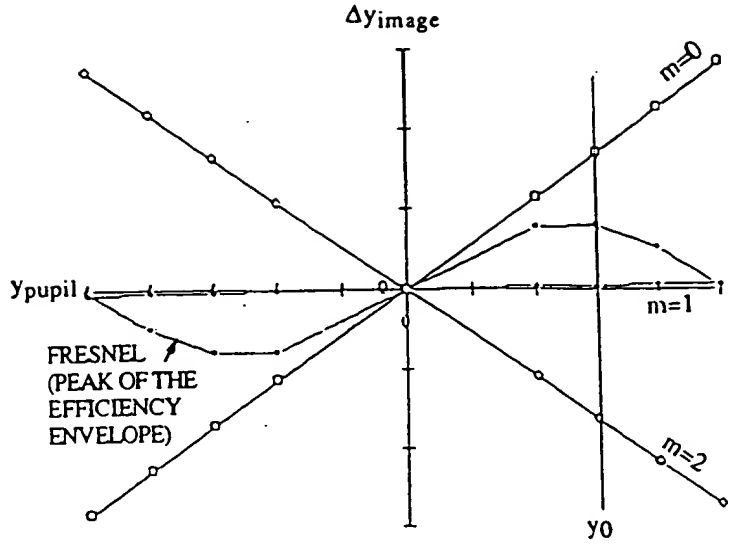

Figure 3. Transverse ray aberrations of the blaze superimposed on those of three diffracted orders.

The second step is to optimize the efficiency of the design order. To optimize efficiency, the system is frozen and the diffractive surface is replaced with a Fresnel surface with the same base curvature. Conventionally, a Fresnel surface has its slope independent of its sag. It is described mathematically by two polynomials with coefficients that are separately variable. One polynomial determines the slope for the light to refract by and the second determines the sagitta.

The slope of the Fresnel surface is varied to optimally match the optical performance of the system with the DOE in place over the design wavelength range and field of view. In general, the Fresnel's performance cannot match the DOE's performance exactly. The best compromise is a balance of efficiency over field and wavelength.

This design method can be extended to systems with multiple DOE's. As previously mentioned, the frequency distributions are designed by simultaneously varying all of the diffractive and conventional elements of the hybrid system. However, the Fresnel surface design to optimize the efficiency must be done separately for each kinoform, with the other DOE's diffracting at the design order and frozen.

6. Image Analysis

An indication of the kinoform's efficiency at several diffracted orders can be obtained by superimposing the transverse aberration plots of these orders on that of the Fresnel surface, as shown in Fig.3. At the image plane, the sinc^2 efficiency envelope is centered on the ray that would be refracted by the Fresnel surface, while the diffracted rays are determined by the hybrid system with the DOE in place. Their relative position within the sinc^2 envelope determines efficiency. As an example, consider the image ray intercept y_0 in Fig.3; the refracted Fresnel "ray" is approximately equidistant to both the zero and first order, so these two orders have nearly the same efficiency.

To quantify the effect on image quality of the light that goes into non-design orders, rays are traced through the hybrid system with the DOE in place. For a single input ray, Fig.4 shows schematically the image ray intercepts for various diffractive orders and the Fresnel surface. To properly weigh each diffraction order by its efficiency, ε_m, the sinc^2 envelope was calculated on a ray by ray basis using equation (6):

$$\varepsilon_m = \text{sinc}^2\left[2\pi \frac{\Delta_{mF}}{\Delta_{02}}\right] \qquad (6)$$

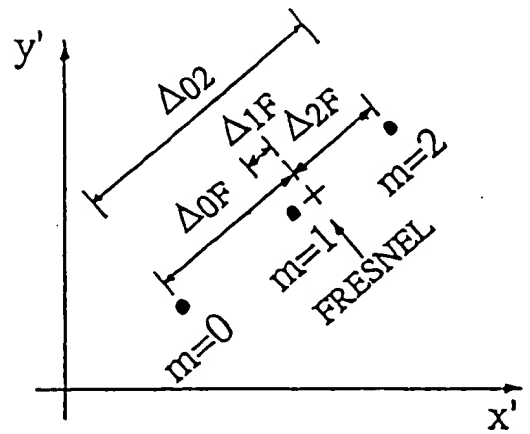

Figure 4. Image coordinates for diffraction efficiency calculation from ray data.

Since the design order is set to m=1, the width of the envelope is the distance between the zero and second order, Δ_{02}. The shift of the envelope is the separation of the diffracted first-order ray and the Fresnel refracted ray, Δ_{1F}. By calculating the efficiency on a ray by ray basis, no approximations are made for changes in geometry, field of view or wavelength. Image quality may be evaluated by tracing a grid of input rays in the entrance pupil for each wavelength and constructing geometric point spread functions (PSF's) from the weighted x,y image coordinates for several diffracted orders.

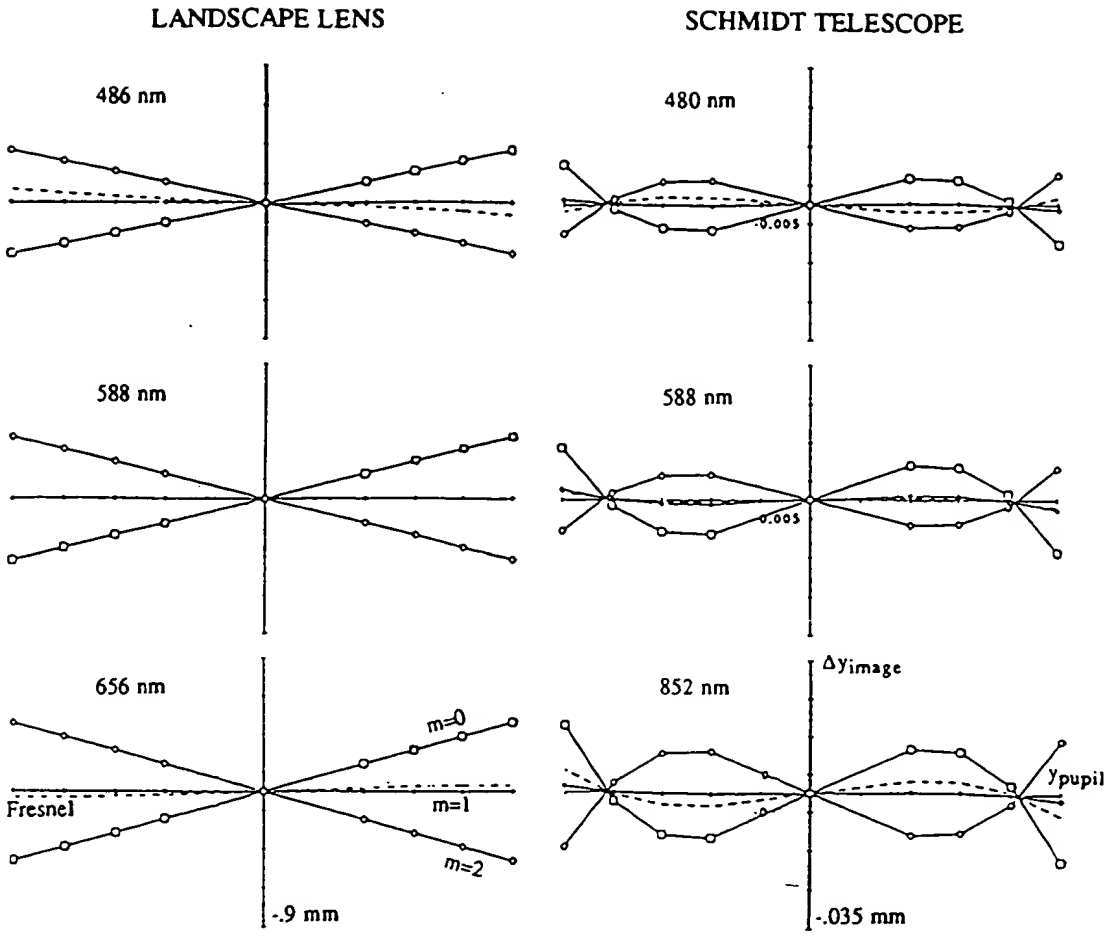

Figure 7. Superimposed transverse aberrations for the on-axis object point.

A measure of efficiency is obtained from Fig.7, which shows the superimposed on-axis transverse aberrations of m=0,1,2 and the Fresnel surface, for the two hybrid systems. Notice that the Fresnel efficiency curve matches the first-order for the central wavelength, but both systems are less efficient at the other wavelengths.

From the weighted x,y image coordinates of orders m=0,1,2, we generated geometric point spread functions (PSF's), line spread functions (LSF's), MTF's, and RMS spot sizes. Ray weights also include factors for wavelength and aperture which, for these examples were set to unity. Note that the PSF's consist of diffracted rays only. The rays traced through the Fresnel surface indicate the center of the efficiency envelope and are not included in the PSF's. Also, when evaluating a system that includes more than one kinoform, there are more combinations of design and non-design orders to choose from when deciding which rays to include in the PSF. For example, if the design order is m=1, one might trace the m=0,1,2 orders for each DOE, with m=1 for the others. So, in a three-DOE system, there may be nine weighted rays in the PSF for each input ray.

The ray-by-ray efficiency calculation described allows us to calculate PSF's with properly weighted rays from a number of diffracted orders. Since it is not always practical to include a large number of orders, the fraction of light that is not included in the PSF is accounted for by assuming that it is diffracted widely across the focal plane, like classical "veiling glare". The fraction of the light that is in the PSF, $\bar{\varepsilon}$, is calculated by dividing the sum of the ray efficiencies by the number of rays in the PSF. This fraction is always less than or equal to one.

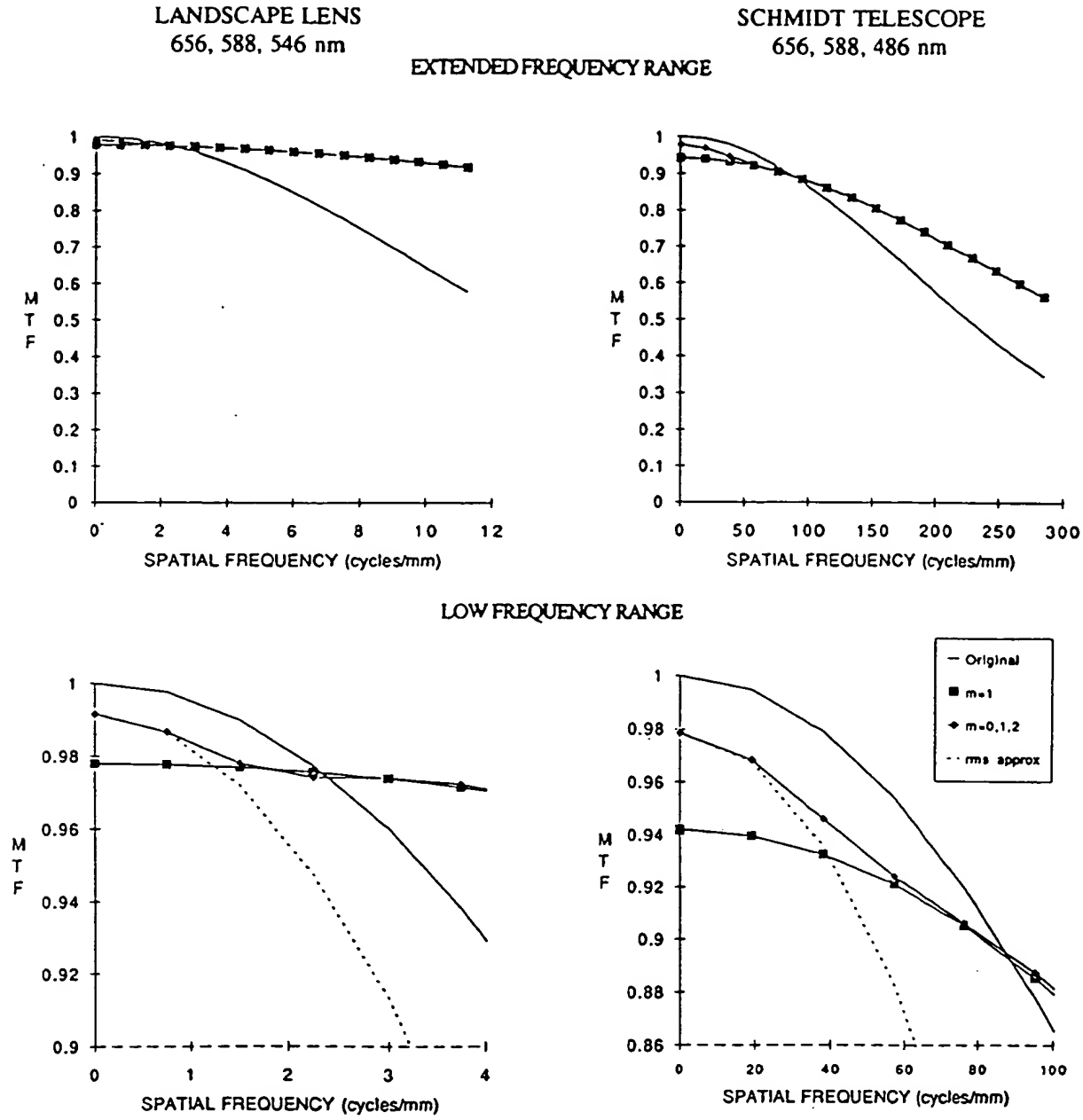

Figure 8. Geometric MTF curves for the on-axis field points.

For example, if the PSF is calculated from rays of order m=0,1,2, $(1-\bar{\varepsilon})$ is the amount of light diffracted into orders other than m=0,1,2. The MTF calculated from this PSF must be corrected for the light that is missing, and is given by:

$$MTF_{corrected} = \bar{\varepsilon}\ MTF_{0,1,2} \tag{7}$$

In general, the total geometrical MTF is the weighted sum of the Fourier transform of the PSF and the MTF of the "veiling glare". In the limit, the MTF of classical veiling glare is an impulse at zero frequency, so the total corrected MTF is approximately the MTF of the PSF, scaled by its efficiency. The veiling glare approximation becomes less valid at low frequencies, because the light diffracted into non-design orders, while severely aberrated, is not really diffracted into an even

Table 1. Geometrical spot sizes and diffraction efficiencies (on-axis).

	LANDSCAPE LENS λ = 656, 588, 546 nm		LANDSCAPE LENS 656, 588, 486 nm		SCHMIDT TELESCOPE 656, 588, 486 nm		SCHMIDT TELESCOPE 852, 588, 480 nm	
	RMS spot size (mm)	Diffraction efficiency	RMS spot size (mm)	Diffraction efficiency	RMS spot size (mm)	Diffraction efficiency	RMS spot size (mm)	Diffraction efficiency
Original	.0203	100	.0279	100	.0009	100	.0014	100
m=1	.0051	97.8	.0025	93.8	.0006	94.2	.0006	81.2
m=0,1,2	.0330	99.2	.0381	97.7	.0012	97.8	.0018	93.7
other orders	-	1.8	-	2.3	-	2.2	-	6.3

background. To make the MTF calculation more accurate at low frequencies, more orders must be included to generate the weighted PSF.

Geometrical MTF curves for the two hybrid systems at two field positions and wavelength ranges were calculated. Since the results were similar, Fig. 8 shows the curves for only one field and one wavelength range. The first curve is the MTF of the original uncorrected system. The second is the MTF calculated from just the design order (m=1) with the other orders treated as veiling glare. The third is the MTF calculated from m=0,1,2 and the residual again treated as veiling glare. The fourth curve is a quadratic approximation to low frequency MTF, which is related to the RMS line spread function size, B_x, by[8]:

$$MTF_x(\nu) = 1 - 2\,\pi^2\,B_x^2\,\nu^2 \tag{8}$$

Thus, the fourth curve was calculated from the RMS line spread function for m=0,1,2, and was likewise corrected for efficiency.

From these figures several observations may be made. First, notice the match between the approximate parabola and the m=0,1,2 MTF curves illustrating the relation between RMS blur and low frequency MTF. Second, for both hybrid designs, the MTF at high frequencies is improved by achromatizing with the kinoform, while the low frequency MTF is actually worse than the uncorrected system. In other words, resolution is increased at the expense of low frequency contrast. Third, notice the agreement between the m=1 and the m=0,1,2 MTF curves at high frequencies. If only the MTF at high frequencies is of interest, the PSF can be simply constructed from design-order rays, treating all other light as veiling glare. It is only when one requires accurate MTF data at low frequencies that the LSF must be refined to include the light that is diffracted into the orders adjacent to the design order.

Table 1 lists the RMS spot sizes and percent energies which correspond to the MTF curves of Fig.8. As one would expect, the percent of light diffracted into non-design orders is smaller for the narrow band systems than for the broadband systems. The RMS spot sizes are improved over the original conventional systems if the design order (m=1) is assumed to be 100% efficient. However, when weighted point spread functions are calculated using orders m=0,1,2, the RMS spot sizes of the achromatized designs are actually larger than the original, indicating reduced MTF's at very low frequencies. Even though there is not much light in the non-design orders, they are highly aberrated and significantly increase the RMS point spread function size.

8. Conclusions

When diffraction efficiency is taken into account, the suitability of achromatized hybrid designs depends upon the spectral bandwidth and upon image quality requirements such as high- versus low-frequency MTF performance. For systems with significant spectral bandwidth, the high frequency response (resolution) can be improved with a hybrid design, but the low frequency response (contrast) may suffer due to the inevitable presence of light in non-design diffracted orders.

Two systems were designed and analyzed using a ray tracing method that includes diffraction efficiency effects in the image quality evaluation. Geometric point spread functions were calculated including properly weighted rays from the design order and several non-design orders. MTF's were then calculated and corrected for the effect of light diffracted into even higher orders.

9. Acknowledgements

Our thanks go to Polaroid Corporation and especially to Dr. William Plummer, Director of Optical Engineering. Also, thanks to many of our colleagues inside and outside of Polaroid for stimulating discussions.

11. References

1. Soret, J.L., "Concerning the Diffraction Phenomena Generated by Means of Circular Gratings", Annalen de Physik, **156**, 99-113 (Poggendorff; 1875).
2. Firth, K., "Recent Developments in Diffractive Optics", GEC Journal of Research, **3**,1 (1985).
3. Buralli, D.A., Morris, G.M., Rogers, J.R., "Optical Performance of Holographic Kinoform", Appl.Opt. **28**, 976 (1989).
4. Hutley, M.C., "Diffraction Gratings", Academic Press, New York (1982).
5. Swanson, G.J., "Binary Optics Technology: The Theory and Design of Multi-Level Diffractive Optical Elements", Technical Report 854, MIT Lincoln Laboratory (1989).
6. "CODE-V" is a registered trademark of Optical Research Associates, Inc., 550 N.Rosemead Blvd., Pasadena CA 91107.
7. Sweatt, W.C., "Describing holographic optical elements as lenses", J.Opt.Soc.Am. **67**, 803 (1977).
8. Plummer, W.T., "Focus screen optimization", Appl.Opt. **14**, 2762 (1975).